Aspects of hyperspherical adiabaticity in an atomic-gas Bose-Einstein condensate

Daisuke Kushibe, Masaki Mutou, Toru Morishita, Shinichi Watanabe, and Michio Matsuzawa
Department of Applied Physics and Chemistry, University of Electro-Communications, 1-5-1, Chofu-ga-oka, Chofu-shi, Tokyo 182-8585, Japan
(Received 3 June 2004; published 20 December 2004)

Excitation of an atomic-gas Bose-Einstein condensate (BEC) in the zeroth-order ground-state channel is studied with the hyperspherical adiabatic method of Bohn *et al.* [Bohn *et al.*, Phys. Rev. A **58**, 584 (1998)] suitably generalized to accommodate the anisotropic trapping potential. The method exploits the system's size as an adiabatic parameter so that the explicit size dependence is immediately conducive to the virial theorem. The oscillation frequencies associated with the monopole (breathing) and quadrupole modes thus emerge naturally and converge to the well-known Thomas-Fermi limits. Analysis of the single-particle density and the projected excitation wave function shows that the excitation in the single hyperspherical ground-state channel merely represents a progressive increase in occupancy of the first excited single-particle state. The work paves the way for applying the adiabatic picture to other BEC phenomena.

DOI: 10.1103/PhysRevA.70.063617 PACS number(s): 03.75.Kk, 03.75.Nt, 05.30.Jp, 03.65.Ge

I. INTRODUCTION

The successful generation of trapped atomic Bose-Einstein condensates in laboratories [1] has opened a new domain of atomic and optical physics, and challenging new phenomena continue to be vigorously explored and regularly reported. Theoretical studies of the phenomena are traditionally based on the mean-field theory due to Bogoliubov [2] which was later cast by Gross and Pitaevskii [3] into the celebrated GP equation. The basic premise of this approach, if stated in simplistic terms, is that the system behaves like a blob of matter representable by a field. This picture has proved so remarkably effective that most observed phenomena are indeed explicable by the GP equation, and conversely no theory tangential to this view has thus far provided as full a description. One of our purposes here is to examine an alternative picture based on the hyperspherical adiabatic method which was applied earlier by Bohn *et al.* [4] to the study of ground-state properties of the Bose-Einstein condensate (BEC) and by Blume and Greene [5,6] to unravel manifolds of adiabatic channels. According to the latter, the BEC channels stand out as the lowest-lying unbound atomic mode whose cohesion is provided singly by the trapping potential. In the wake of such development, it appears natural to ask in what aspects the GP and the hyperspherical picture coincide or differ apart from the obvious differences in the ground state. This inquiry serves as a purpose of this paper.

Incidentally, the hyperspherical adiabatic method was originally proposed by Macek [7] in 1968 for analyzing the dynamical features of doubly excited states of He, and since then, it has been promoted by Fano and others [8] in order to visualize the dynamics of three- and four-body systems [9]. The point of departure from the traditional adiabatic viewpoint of molecular physics is the choice of adiabatic variables. Macek recognized the special role played by the root-mean-square size of the system, the hyperradius, as the system's distinctive adiabatic variable. This approach has seen a great deal of success in various facets of few-body systems in the past three decades [10].

We should state at the outset that parametrization of the solution by the Gaussian wave-packet ansatz such as in Ref. [11] is along the line of our adiabatic approach for they reformulate the problem by integrating out rapidly varying dynamical variables. On the other hand, in the hyperspherical method the adiabatic variables play a more distinct role in the spirit of the Born-Oppenheimer treatment of molecules. Excitations with respect to the adiabatic degrees of freedom are thus within the natural scope of the hyperspherical method while quantization with respect to the parameters of the other treatment such as Ref. [11] would require further qualification.

Many of the recent works concern not only the collective modes [12] of BEC's but phenomena such as interference between different types of BEC's [13], collapse of a BEC with attractive interparticle interaction [14], vortices both topological [15] and nontopological [16], spin degrees of freedom [17], and solitons [18]. We wish, however, to focus on the following issues in the subsequent sections, leaving other applications to separate articles.

(i) We generalize the hyperspherical method of Ref. [4] to an anisotropic trap (Sec. II).

(ii) We discuss the collective oscillations studied previously by Stringari [19] and other workers [20], recasting them into the context of the hyperspherical representation (Sec. III).

(iii) We analyze the nature of the hyperspherical excitations in the ground-state channel, comparing them to the independent particle picture (Sec. IV). This requires us to generalize the formula in Ref. [4] for the particle density.

Furthermore, an analytical procedure for the evaluation of matrix elements with respect to hyperspherical harmonics is reconsidered in the Appendix for the purpose of a pedagogical illustration. Using a generating function method for calculating several lowest-order hyperspherical harmonics, we demonstrate an energy shift, if miniscule, of the ground state due to the coupled hyperspherical channels in Sec. III. A subsection also in Sec. III complements the hyperspherical estimate of the ground state's total energy on the basis of the Thomas-Fermi approximation to the GP equation. Note we employ the δ-function-type effective potential throughout unlike the Blume-Greene paper [5]. No recombination chan-

nels thus appear explicitly in this work. Oscillator units (o.u.) [21] will be used unless stated otherwise.

II. GENERALIZED HYPERSPHERICAL FRAMEWORK FOR BEC'S

The full Hamiltonian of N identical bosons of mass m confined in a harmonic oscillator potential of a magneto-optical trap reads

$$H = T_G + T + V_{\text{trap}} + V_{\text{int}},$$

where T_G is the kinetic energy operator of the center of mass, T is that of the BEC in the center-of-mass frame given by

$$T = -\frac{\hbar^2}{2m}\sum_{i=1}^{N}\nabla_i^2,$$

and the trapping potential V_{trap} is, owing to its harmonicity,

$$V_{\text{trap}} = \frac{1}{2}m\sum_{i=1}^{N}(\omega_x^2 x_i^2 + \omega_y^2 y_i^2 + \omega_z^2 z_i^2) + \frac{1}{2}M(\omega_x^2 X_G^2 + \omega_y^2 Y_G^2 + \omega_z^2 Z_G^2).$$

Here, ω_x, ω_y, and ω_z are the trap frequencies in the x, y, and z directions, respectively. The center-of-mass motion separates out to perform a three-dimensional (3D) harmonic motion with frequencies $\{\omega_x, \omega_y, \omega_z\}$. From hereafter, we limit ourselves to where the center of mass coincides with the potential minimum—that is, where

$$X_G = Y_G = Z_G = 0.$$

The interaction of pairs of atoms is represented by the short-range δ-function potential parametrized by the s-wave scattering length a:

$$V_{\text{int}} = \frac{4\pi\hbar^2}{m}a\sum_{i>j}\delta(\vec{r}_i - \vec{r}_j).$$

We use the parameter

$$g = \frac{4\pi\hbar^2}{m}a$$

hereafter to represent the strength of interaction. We shall now outline the procedure for the hyperspherical adiabatic expansion and deduce an effective potential in the lowest-order hyperspherical harmonics approximation. We shall refer to this approximation as the K-harmonic approximation (KHA) [4] and distinguish it from the hyperspherical adiabatic method designed for few-body systems [7–9]. In so doing, let us modify the standard hyperspherical method to accommodate the nonisotropic trapping potential. Otherwise, the treatment is closely in line with Ref. [4].

The elliptically anisotropic case of $\omega_x = \omega_y = \omega_\rho \neq \omega_z$ has all the essential elements for further generalization. Here the trapping potential reads

$$V_{\text{trap}} = \frac{1}{2}m\sum_{i=1}^{N}(\omega_\rho^2\rho_i^2 + \omega_z^2 z_i^2) = \frac{1}{2}mN(\omega_\rho^2 R_\rho^2 + \omega_z^2 R_z^2),$$

where $\rho_i^2 = x_i^2 + y_i^2$ and the hyperradii are defined by

$$R_\rho^2 = \frac{1}{N}\sum_{i=1}^{N}\rho_i^2,$$

$$R_z^2 = \frac{1}{N}\sum_{i=1}^{N}z_i^2.$$

(For the most general situation, R_x, R_y, and R_z may be similarly defined.) The kinetic energy operator reads

$$T = -\frac{\hbar^2}{2mN}\left(\frac{1}{R_\rho^{2N-1}}\frac{\partial}{\partial R_\rho}R_\rho^{2N-1}\frac{\partial}{\partial R_\rho} - \frac{\Lambda_\rho^2}{R_\rho^2} + \frac{1}{R_z^{N-1}}\frac{\partial}{\partial R_z}R_z^{N-1}\frac{\partial}{\partial R_z} - \frac{\Lambda_z^2}{R_z^2}\right),$$

where Λ_ρ and Λ_z are the grand angular momentum operators associated with the rotational degrees of freedom on the R_ρ and R_z hyperspheres, respectively. The specific expression for Λ^2 in d dimensions is

$$\Lambda^2 = -\sum_{i>j}^{d}\left(\xi_i\frac{\partial}{\partial\xi_j} - \xi_j\frac{\partial}{\partial\xi_i}\right)^2,$$

where the set of variables $\{\xi_i\}$ represent the Cartesian coordinates in a d-dimensional space [22,26]. We consider the hyperspherical harmonics—namely, the eigenvectors of the grand angular momentum operator—as a basis set for expansion. Let us write, symbolically,

$$\Lambda_\rho^2\mathcal{Y}_{\{\lambda_\rho\}}^{\rho}(\Omega_\rho) = \lambda_\rho(\lambda_\rho + 2N - 2)\mathcal{Y}_{\{\lambda_\rho\}}^{\rho}(\Omega_\rho),$$

$$\Lambda_z^2\mathcal{Y}_{\{\lambda_z\}}^{z}(\Omega_z) = \lambda_z(\lambda_z + N - 2)\mathcal{Y}_{\{\lambda_z\}}^{z}(\Omega_z),$$

where Ω_ρ and Ω_z represent the angular degrees of freedom on the two hyperspheres. These equations are largely indicative of the dimensionality of the Hilbert spaces; the order of harmonics for each degree of freedom is given by

$$\lambda_\rho(\lambda_z) = 0, 1, 2, \ldots .$$

Likewise the sets of quantum numbers are conveniently symbolized here by a curly-bracketed index pertaining to the totality of nodes in the wave function—namely, $\{\lambda_\rho\}$ and $\{\lambda_z\}$—while quantum numbers that distinguish degenerate subcomponents are to be thus understood implicitly.

The solution $\Psi(R_\rho, R_z; \Omega_\rho, \Omega_z)$ of the Schrödinger equation may be expressed in terms of the sum of direct products,

$$\Psi(R_\rho, R_z; \Omega_\rho, \Omega_z) = N^{3N/4}R_\rho^{(2N-1)/2}R_z^{(N-1)/2}\sum_{\{\lambda_\rho\},\{\lambda_z\}}F_{\{\lambda_\rho\},\{\lambda_z\}} \times (R_\rho, R_z)\mathcal{Y}_{\{\lambda_\rho\}}^{\rho}(\Omega_\rho)\mathcal{Y}_{\{\lambda_z\}}^{z}(\Omega_z), \quad (1)$$

where the coefficients $\{F_{\{\lambda_\rho\},\{\lambda_z\}}(R_\rho, R_z)\}$ hold the key to the BEC's bulk dynamics while R_ρ and R_z are treated as constant

parameters when defining the adiabatic potential surfaces, and the factor $R_\rho^{(2N-1)/2}R_z^{(N-1)/2}$ is introduced here to simplify the kinetic energy operator. There are alternative ways to define expansion basis functions which would allow for the distortion of the system under the interaction potential. Details of such alternatives are skipped to avoid sidetracking the main purpose; the reader is invited to the review by Fano [23]. The hyperradial equation is then expressed as

$$\left[-\frac{\hbar^2}{2mN}\left\{\frac{\partial^2}{\partial R_\rho^2}-\frac{(2N-1)(2N-3)/4+\lambda_\rho(\lambda_\rho+2N-2)}{R_\rho^2}+\frac{\partial^2}{\partial R_z^2}-\frac{(N-1)(N-3)/4+\lambda_z(\lambda_z+N-2)}{R_z^2}\right\}+V_{\rm trap}\right]\times F_{\{\lambda_\rho\},\{\lambda_z\}}(R_\rho,R_z)+\sum_{\{\lambda_\rho'\},\{\lambda_z'\}}\langle\langle\mathcal{Y}^\rho_{\{\lambda_\rho\}}\mathcal{Y}^z_{\{\lambda_z\}}|V_{\rm int}|\mathcal{Y}^\rho_{\{\lambda_\rho'\}}\mathcal{Y}^z_{\{\lambda_z'\}}\rangle\rangle\times F_{\{\lambda_\rho'\},\{\lambda_z'\}}(R_\rho,R_z)=EF_{\{\lambda_\rho\},\{\lambda_z\}}(R_\rho,R_z),$$

where double angular brackets $\langle\langle\ldots\rangle\rangle$ indicate integration with respect to the hyperangles Ω_ρ and Ω_z. Note that the orthonormality of the hyperspherical harmonics is used. A simple dimensional consideration on the δ function readily reveals that the interaction term is inversely proportional to the volume—namely,

$$\langle\langle\mathcal{Y}^\rho_{\{\lambda_\rho\}}\mathcal{Y}^z_{\{\lambda_z\}}|V_{\rm int}|\mathcal{Y}^\rho_{\{\lambda_\rho'\}}\mathcal{Y}^z_{\{\lambda_z'\}}\rangle\rangle\propto\frac{1}{R_\rho^2R_z}.$$

Though techniques for evaluating various matrix elements are besides the point in the current paper, we spare an appendix for outlining a simple procedure. It yields, in the KHA [i.e., the terms with $\lambda_\rho=\lambda_z=0$ only in Eq. (1)],

$$\langle\langle\mathcal{Y}^\rho_{\{0\}}\mathcal{Y}^z_{\{0\}}|V_{\rm int}|\mathcal{Y}^\rho_{\{0\}}\mathcal{Y}^z_{\{0\}}\rangle\rangle=\frac{G_0^{\rho z}}{R_\rho^2R_z}.$$

The interaction constant simplifies to

$$G_0^{\rho z}=\frac{g}{(2\pi)^{3/2}}\frac{N(N-1)}{2}\left(\frac{\Gamma(N)}{N\Gamma(N-1)}\frac{\Gamma\left(\frac{N}{2}\right)}{N^{1/2}\Gamma\left(\frac{N-1}{2}\right)}\right),$$

which behaves as

$$G_0^{\rho z}\simeq\frac{g}{4\pi^{3/2}}\frac{N(N-1)}{2},$$

when $N\gg1$. The effective hyperspherical potential energy $V_{\rm eff}(R_\rho,R_z)$ is the sum of the pseudocentrifugal potential, $V_{\rm trap}$ and $V_{\rm int}$—namely,

$$V_{\rm eff}(R_\rho,R_z)=\frac{\hbar^2}{8mN}\left\{\frac{(2N-1)(2N-3)}{R_\rho^2}+\frac{(N-1)(N-3)}{R_z^2}\right\}+\frac{1}{2}mN(\omega_\rho^2R_\rho^2+\omega_z^2R_z^2)+\frac{G_0^{\rho z}}{R_\rho^2R_z}.\quad(2)$$

Incidentally, deduction of the effective potential is as straightforward for the general case of R_x, R_y, and R_z. We have

$$V_{\rm eff}(R_x,R_y,R_z)=\frac{\hbar^2}{2m}\frac{(N-1)(N-3)}{4N}\left(\frac{1}{R_x^2}+\frac{1}{R_y^2}+\frac{1}{R_z^2}\right)+\frac{1}{2}mN(\omega_x^2R_x^2+\omega_y^2R_y^2+\omega_z^2R_z^2)+\frac{G_0^{xyz}}{R_xR_yR_z},$$

where

$$G_0^{xyz}=\frac{g}{(2\pi)^{3/2}}\frac{N(N-1)}{2}\frac{\Gamma\left(\frac{N}{2}\right)^3}{N^{3/2}\Gamma\left(\frac{N-1}{2}\right)^3}.$$

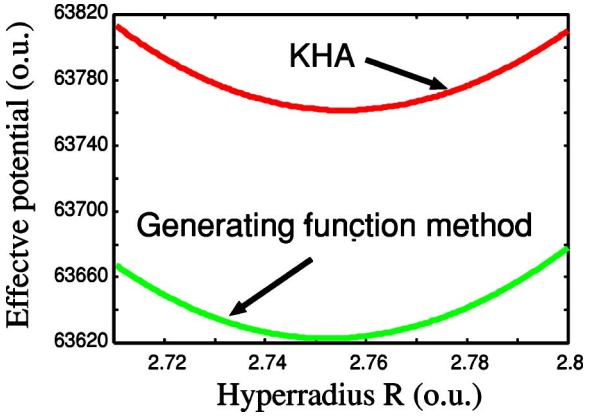

FIG. 1. Ground-state channel potential curves for $N=1000$ by the KHA and by the generating function method. Eleven hyperspherical harmonics are used for the latter. o.u. denotes oscillator units.

III. GROUND-STATE CHANNEL AND COLLECTIVE MODES

In this section, we consider collective modes in an isotropic trap. The generalization of the KHA to the anisotropic trap as presented in the previous section serves to identify modes that do not emerge in the strictly isotropic formulation. However, before going into the discussion of the collective modes, we digress on the total energy of the system, first by coupling several channels and second by a Thomas-Fermi-type approximation.

A. Several hyperpherical channels and total energy of an isotropic BEC

Knowledge of the matrix elements of the grand angular momentum operator leads to the desired hyperspherical harmonics for an N-particle system by way of diagonalization. An estimate of the ground-state energy provides an illustration of this sequence of calculations though we only achieve a marginal improvement. Indeed, using 11 low-lying hyperspherical harmonics generated with the type-B generating function in the Appendix, naturally we observe the lowering of the adiabatic potential curves as depicted in Fig. 1. Figure

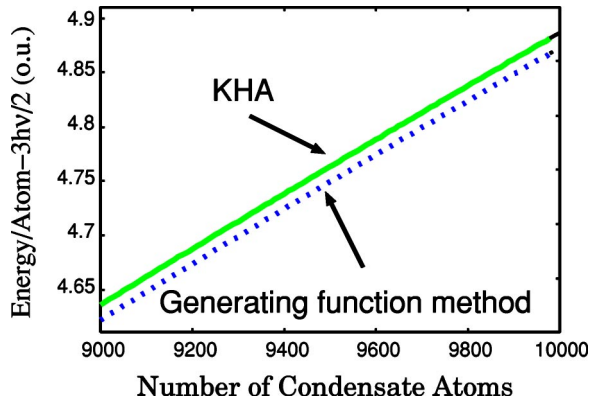

FIG. 2. Ground-state energy per particle minus $\frac{3}{2}\hbar\omega(\frac{3}{2}h\nu)$ as a function of N. The solid line is for the case of a single hyperspherical harmonics and the dashed line for 11 hyperspherical harmonics.

2 shows some ground-state energy per particle $-\frac{3}{2}\hbar\omega$; inclusion of other hyperspherical harmonics does not lead to a substantial lowering of the total energy. The shift remains about one order of magnitude smaller than the difference between the Hartree-Fock-type approximation and KHA at, say, $N=5000$. This result is not unexpected, of course, since the direct product anzatz for the wave function as tacitly assumed for the GP equation is equivalent to a factorially large number of terms in the direct sum representaion as pertains to the perturbative expansion based on the harmonics. Thus, by the present method we expect resonable improvement only for a system with a small number of atoms. A slight improvement on the estimate of the total energy is afforded by the Hartree-Fock estimate of the hyperspherical interaction energy using the constrained Thomas-Fermi solution.

B. Hartree-Fock-type estimate of the hyperspherical interaction potential

In a field-theoretic picture, the hyperspherical radius may be viewed as a dynamical constraint on the system, and its operatorial representation in terms of the field operator $\hat{\phi}(\vec{r})$ may be given by

$$\hat{R}^2 = \int \hat{\phi}^\dagger(\vec{r})\vec{r}^2\hat{\phi}(\vec{r})d\vec{r}.$$

We demand that its expectation value be fixed to a c number R^2. The Hartree-Fock-type equation of motion, a slightly modified version of the GP equation, can be deduced with the aid of the Lagrange multiplier—namely,

$$-\frac{\hbar^2}{2m}\nabla^2\phi + \frac{1}{2}m\omega^2r^2\phi + g|\phi|^2\phi + \lambda r^2\phi = \mu\phi,$$

where $\phi(\vec{r})$ is the mean-field ground-state function and μ is the chemical potential. The Lagrange multiplier is determined by the condition

$$\int r^2|\phi(\vec{r})|^2d\vec{r} = \tilde{R}^2,$$

while μ is fixed by the normalization

$$\int |\phi(\vec{r})|^2d\vec{r} = N.$$

Once the solution ϕ obtains, the total energy follows from

$$E = N\int \phi^*(\vec{r})\left\{-\frac{\hbar^2}{2m}\nabla^2 + V_{\text{trap}}(\vec{r}) + \frac{g}{2}(N-1)|\phi(\vec{r})|^2\right\} \times\phi(\vec{r})d\vec{r}.$$

Applying the Thomas-Fermi approximation to the modified GP equation, we obtain the solution

$$\phi_{\text{TF}}(\vec{r}) = \sqrt{\frac{1}{g}\left(\mu - \frac{1}{2}m\omega^2r^2 - \lambda r^2\right)},$$

where $\mu=(15N_g/8\pi)(\frac{3}{7})^{3/2}(1/\tilde{R}^3)$ and $\lambda=\frac{1}{2}-3\mu/7\tilde{R}^3$ in o.u. The total energy E_{TF} reads

$$E_{\text{TF}} = N\int \phi^*(\vec{r})\left\{V_{\text{trap}}(\vec{r}) + \frac{g}{2}(N-1)|\phi(\vec{r})|^2\right\}\phi(\vec{r})d\vec{r}$$
$$= \frac{1}{2}mN\omega^2\tilde{R}^2 + \frac{N(N-1)}{2}g\frac{30}{7}\left(\frac{3}{7}\right)^{3/2}\frac{1}{4\pi}\frac{1}{\tilde{R}^3}.$$

The numerical coefficient in the last term is given by

$$\frac{1}{4\pi}\frac{30}{7}\left(\frac{3}{7}\right)^{3/2} = 0.0957,$$

which is to be compared to the corresponding hyperspherical coefficient

$$\frac{\xi}{\sqrt{8\pi^3}} \simeq 0.117.$$

The Thomas-Fermi estimate is thus about 20% smaller than that of the KHA approximation.

Incidentally, direct use of the Gaussian approximation [27] to ϕ, namely,

$$\phi(\vec{r}) = \left(\frac{3}{2\pi}\right)^{3/4}\frac{1}{\tilde{R}^{3/2}}\exp\left(-\frac{3r^2}{2\tilde{R}^2}\right),$$

leads to

$$E_g[\tilde{R}] = \frac{\hbar^2}{2m}\frac{9N}{4\tilde{R}^2} + \frac{1}{2}mN\omega^2\tilde{R}^2 + \frac{N(N-1)}{2}\left(\frac{3}{2}\right)^{3/2}\frac{g}{\sqrt{8\pi^3}}\frac{1}{\tilde{R}^3},$$

which coincides, not surprisingly, with the hyperspherical potential energy in the $N\gg1$ limit.

C. Collective modes in the KHA

Let us now recall that we consider the case where the center of mass is located at the center of the trap. The hyperradius $R=\sqrt{R_\rho^2+R_z^2}$ then represents the effective size of the system so that its departure from the local minimum of the potential corresponds to the expansion and contraction of the system—i.e., the breathing motion (monopole). A mode orthogonal to the breathing also exists under the constraint of

R=const.—namely, the quadrupole mode as we shall see despite the crudeness of the KHA.

The KHA leads to the two-dimensional partial differential equation

$$\left[-\frac{\hbar^2}{2m}\left(\frac{\partial^2}{\partial R_\rho^2}+\frac{\partial^2}{\partial R_z^2}\right)+V_{\rm eff}(R_\rho,R_z)\right]F_{\{0\},\{0\}}(R_\rho,R_z)$$
$$=EF_{\{0\},\{0\}}(R_\rho,R_z). \quad (3)$$

Before going into a discussion of the limiting cases of $N\sim 1$ and $N\gg 1$, we diagonalize Eq. (3) above numerically. This then results in energy levels and, hence, excitation energies. With ^{87}Rb as a specific example of atomic species for BEC's for which the scattering length $a\simeq 100$ bohrs, Fig. 3 shows several lowest excitation energies of a ^{87}Rb BEC in the isotropic limit where ω_ρ and $\omega_z\to\omega=2\pi\times 200$ Hz. This result should be compared with Fig. 3 of Ref. [4].

A couple of features that we read off from Fig. 3 are first in the $N\simeq 1$ regime the excitation energies are multiples of 2ω as should be for a three-dimensional harmonic oscillator. In the $N\gg 1$ regime the KHA yields intercombination lines of the form $(\sqrt{5}n_1+\sqrt{2}n_2)\omega$ [Fig. 3(b)] where $\sqrt{5}\omega$ and $\sqrt{2}\omega$ pertain to the asymptotic limits of the breathing and quadrupole oscillations, respectively [24]. Let us now compare this result to the excitation energies evaluated numerically by solving the Bogoliubov equation [25] in Fig. 3(a). In the Bogoliubov approximation, the calculated states are of even parity and restricted to those which coincide with the KHA states at $N=1$. They are continued smoothly across anticrossings to maintain their nodal structures. We observe that besides those that converge rather quickly to the asymptotic limits some continue to fall, crossing those which have already attained their limits. A point of the discussion to follow is to identify the origin of this departure.

Incidentally, Fig. 3(c) expands the region between $N=1$ and $N=3000$ (both the ordinate and abscissa are expanded), displaying the KHA results (solid lines) and the Bogoliubov results (dashed lines). This is the region where the difference in estimate of the effective coupling strength $G_0^{\rho z}$ becomes slightly visible. The KHA overestimates $G_0^{\rho z}$ so that the excitation energies become slightly more widely separated. (An alternative estimate of $G_0^{\rho z}$ based on the Thomas-Fermi approximation to the GP equation is previously discussed in Sec. III B, which estimate is also slightly smaller.) The scaling property [26] is an important aspect of the trapped atomic BEC, the excitation frequencies $\sqrt{5}\omega$ and $\sqrt{2}\omega$ of the monopole and quadrupole modes being a direct consequence of this. To see their manifestation, let us note that the kinetic energy scales as R^{-2}, the trapping potential as R^2, and the bulk interaction as R^{-3}. The *virial theorem* [24] is thus explicit in the hyperspherical representation—that is,

$$2E_{\rm kin}-2E_{\rm trap}+3E_{\rm int}=0.$$

Note the kinetic energy has two parts: one is the hyperradial kinetic energy operator and the other is the effective potential varying as R^{-2}. The $N\gg 1$ approximation about to be applied neglects the latter only, keeping the virial theorem intact in spite of the absence of the kinetic energy term in the effective potential. In other words, the proper quantization is retained on account of the hyperspherical kinetic energy operator. Though this regime $N\gg 1$ is obviously beyond the scope of the KHA, the scale-dependent features turn out insensitive to the details of the description. The excitation frequencies start off with the multiples of 2ω near $N=1$; then, a Thomas-Fermi [24] type behavior sets in toward $N\gg 1$ where Eq. (2) is approximated by

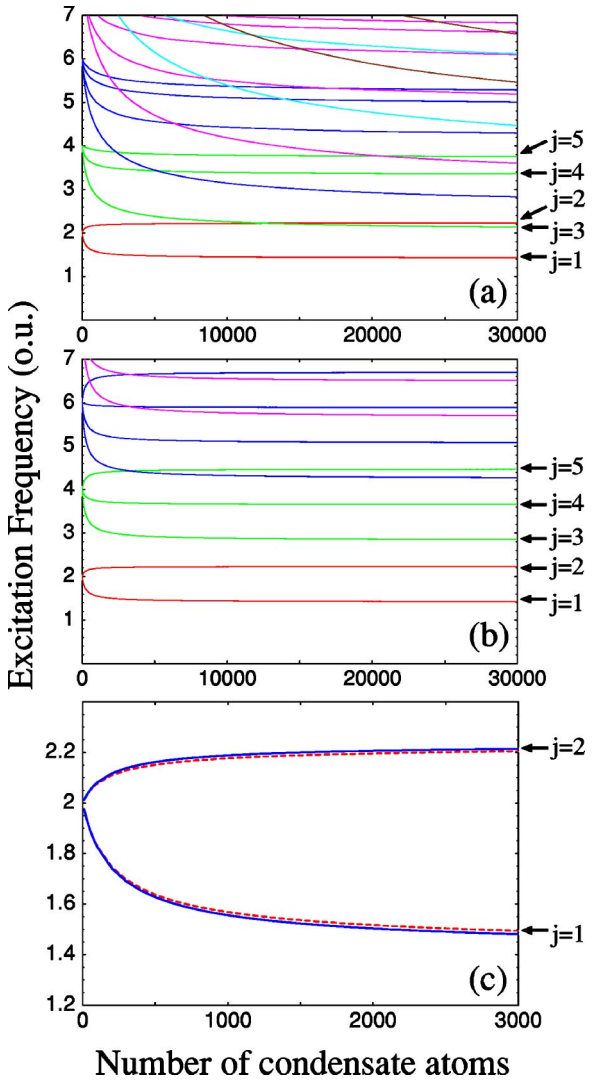

FIG. 3. Excitation frequencies of ^{87}Rb as a function of number of particles N with $a=100$ bohrs and $\omega_\rho=\omega_z=2\pi\times 200$ Hz. (a) In the Bogoliubov approximation and (b) in the KHA approximation. For the former (a), the calculated states are of even parity and restricted to those which coincide with the KHA states at $N=1$. Index j labels them from low to high at $N\simeq 1$. This labeling is continued across the anticrossings to maintain the correspondence of eigenmodes as N grows. In the large-N limit, excitation energies of breathing and quadrupole modes are approximately $\sqrt{5}n_1$ and $\sqrt{2}n_2$ in the KHA, respectively, so that combinations of the form $\sqrt{5}n_1+\sqrt{2}n_2$ occur where n_1 and n_2 are integers. In the Bogoliubov case, there occur modes whose excitation frequencies continue to lower after the KHA results have converged to their asymptotic limits. (c) Comparison of (a) and (b) on an expanded scale (both abscissa and ordinate) for the lowest two excitation frequencies.

$$V_{\rm eff}(R_\rho,R_z) \simeq \frac{1}{2}m(\omega_\rho^2 R_\rho^2 + \omega_z^2 R_z^2) + \frac{G_0^{\rho z}}{R_\rho^2 R_z}.$$

This effective potential coincides in form with Eq. (13) of Ref. [11] derived from the viewpoint shared by Ref. [27]. The specific value of the interaction constant $G_0^{\rho z}$ depends on the employed method and approximations. The procedure for determining the collective excitation frequency ω is first to locate the minimum of the potential well by setting the first-order derivatives to zero. Then the eigenvalues of the Hessian matrix $\mathcal{K}$ are sought where

$$\mathcal{K} = \frac{1}{2}\begin{pmatrix} \dfrac{\partial^2 V_{\rm eff}}{\partial R_\rho^2} & \dfrac{\partial^2 V_{\rm eff}}{\partial R_\rho \partial R_z} \\ \dfrac{\partial^2 V_{\rm eff}}{\partial R_z \partial R_\rho} & \dfrac{\partial^2 V_{\rm eff}}{\partial R_z^2} \end{pmatrix}_{R_\rho = R_{\rho 0}, R_z = R_{z0}},$$

and $R_{\rho 0}$ and R_{z0} are the coordinates of the potential minimum. The eigenvalues yield the curvatures of the potential near the minimum, and the collective coordinates are identified by the eigenvectors. The result is as in [19]:

$$\omega_\mp^2 = 2\omega_\rho^2 + \frac{3}{2}\omega_z^2 \mp \frac{1}{2}\sqrt{9\omega_z^4 - 16\omega_z^2\omega_\rho^2 + 16\omega_\rho^4}.$$

The corresponding eigenvectors $v_\mp$ are $v_- = \sqrt{\frac{1}{3}}(\sqrt{2},1)$ and $v_+ = \sqrt{\frac{1}{3}}(-1,\sqrt{2})$ so that the first pertains to the breathing and the other to the quadrupole mode. In going through this exercise, one realizes that the interaction constant $G_0^{\rho z}$ cancels out, thus bringing out the features only dependent on the dimensionality of the problem, hence allowing even a crudest approximation to reproduce the experimentally observed frequencies correctly. The reliability of a theory must then be sought and questioned in the context of other physical quantities explicitly dependent on all the terms in the Hamiltonian.

Let us recapitulate the result on hand. We have employed only the lowest hyperspherical harmonics which is constant over each hypersphere and represents the totally symmetric states of the aggregates of bosons. The ρ and z degrees of freedom initially treated as though decoupled are brought into correlation via the particle density term. The breathing and quadrupole modes emerged, and their lowest excitation frequencies agreed with the Bogoliubov results. The so-called "ballistic" treatment [11] based on the Gaussian wave packet is similar in spirit in that the curvature of the local effective potential plays a key role. In the present adiabatic picture, the effective potential emerges more naturally since the boundary condition on the wave function (or a certain phase factor) need not be explicitly specified. From the viewpoint that the hyperradii represent the mean-square size of the system in each dimension, the present result is not unanticipated. However, the excitation in each adiabatic mode represents on one hand a collective oscillation frequency and on the other hand a quantum mechanical and rather diminutive excitation energy. These somewhat disparate ideas need to be reconciled. We examine excitations more closely in the next section and, in particular, characterize the modes with slowly converging excitation frequencies.

IV. EXCITATION IN THE GROUND-STATE CHANNEL

Though inclusion of excited adiabatic channels is formally possible using the generating function techniques of the Appendix, we focus here only on aspects of the single-channel excitation in the KHA. To this end, we evaluate the single-particle density $n_j(\rho,z)$ as well as the effective single-particle excited state wave function $\chi_j(\rho,z)$ and take the isotropic limit. These functions are defined by the matrix element

$$n_j(\rho,z) = \left\langle F_j^{(N)}(R_\rho,R_z)\mathcal{Y}_{\{0\}}^{(N)}(\Omega_\rho)\mathcal{Y}_{\{0\}}^{(N)}(\Omega_z) \left| \sum_{k=1}^{N} \delta(\vec{r}-\vec{r_k}) \right| F_j^{(N)} \times (R_\rho,R_z)\mathcal{Y}_{\{0\}}^{(N)}(\Omega_\rho)\mathcal{Y}_{\{0\}}^{(N)}(\Omega_z) \right\rangle_N \quad (4)$$

and by the projection

$$\chi_j(\rho,z) = \langle F_0^{(N-1)}(R_\rho^{(N-1)},R_z^{(N-1)})\mathcal{Y}_{\{0\}}^{(N-1)}(\Omega_\rho)\mathcal{Y}_{\{0\}}^{(N-1)}(\Omega_z)|F_j^{(N)} \times (R_\rho^{(N)},R_z^{(N)})\mathcal{Y}_{\{0\}}^{(N)}(\Omega_\rho)\mathcal{Y}_{\{0\}}^{(N)}(\Omega_z)\rangle_{N-1}, \quad (5)$$

respectively, and here we have the relationship

$$R^{(N)2} = \frac{N-1}{N}R^{(N-1)2} + \frac{1}{N}r^{(N)2}.$$

In Eqs. (4) and (5), the suffixes in the brackets $\langle\cdots\rangle_N$ and $\langle\cdots\rangle_{N-1}$ denote integrations with respect to the coordinates of the N- and $(N-1)$-particle systems, respectively. The function $\chi_j(\rho,z)$ is thus nothing but the projection of an excited state eigenfunction onto the ground-state wave function of the $(N-1)$-particle system. Incidentally, the projected excitation function $\chi = \langle \Psi_0^{(N-1)} | \Psi_j^{(N)} \rangle_{N-1}\rangle$, where $\Psi_0^{(N-1)}$ is the ground-state function of the $(N-1)$-particle system, satisfies the equation

$$\left\langle \Psi_0^{(N-1)} \left| -\frac{\hbar^2}{2m}\nabla^2 + \frac{1}{2}m\omega^2 r^2 + g\sum_{i=1}^{N-1}\delta(\vec{r_i}-\vec{r}) \right| \Psi_j^{(N)} \right\rangle_{N-1} = (E_j^{(N)} - E_0^{(N-1)})\chi,$$

where $\vec{r}$ pertains to the Nth particle. In the frozen core approximation, we have

$$-\frac{\hbar^2}{2m}\nabla^2\chi + \frac{1}{2}m\omega^2 r^2\chi + (N-1)g\rho^{(N-1)}(\vec{r})\chi = \mu\chi,$$

with $\mu = E_j^{(N)} - E_0^{(N-1)}$ where $\rho^{(N-1)}(\vec{r})$ is the particle density of the $(N-1)$-particle system in its ground state while the GP direct product ansatz for $\Psi^{(N-1)}$ reduces it to the GP equation. What we do below is an explicit extraction and interpretation of χ in the KHA approximation.

It is worth noting that both $n_j(\rho,z)$ and $\chi_j(\rho,z)$ can be evaluated by two-dimensional integrals—that is,

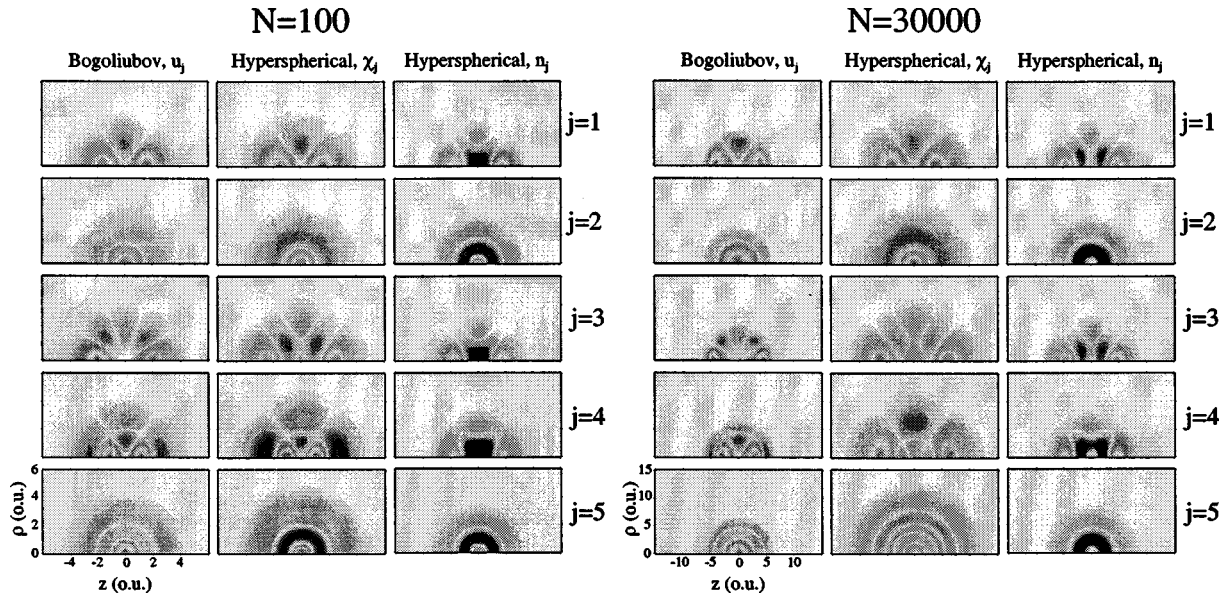

FIG. 4. Comparison of the projected single-particle excitation function χ_j and the Bogoliubov function u_j for $N=100$ and 30 000. The abscissa is z and the ordinate is ρ. Hyperspherical density n_j is also shown. For the rather small BEC of $N=100$, χ_j and u_j resemble one another in terms of their major features except for sextupole, $j=3$. Observe the radial (monopole) excitation from $j=1$ to $j=4$ and also from $j=2$ to $j=5$. For $N=30\,000$, the Thomas-Fermi-type behavior for u_j and the Gaussian behavior for χ_j become more discernible. Angular features continue to show resemblance except for $j=3$. As for the hyperspherical density, the pattern of resemblance seen between χ_j and u_j is now absent from n_j except for $j=2$. The pattern of correspondence is now δn_2 to δn_5 and δn_1 to δn_3 instead of δn_1 to δn_4. The nodal structures of these pairs remain identical as N changes, thus no increment in number of nodes.

$$n_j(\rho,z) = \frac{\xi N}{\pi^{3/2}} \int_{\rho/\sqrt{N}}^{\infty} \int_{|z|/\sqrt{N}}^{\infty} \frac{|F_j^{(N)}(R_\rho,R_z)|^2}{R_\rho^2 R_z} \left(1 - \frac{\rho^2}{NR_\rho^2}\right)^{N-2} \times \left(1 - \frac{z^2}{NR_z^2}\right)^{(N-3)/2} dR_\rho dR_z \tag{6}$$

and

$$\chi_j(\rho,z) = \left(\frac{1}{\pi}\right)^{3/4} \sqrt{\frac{N\xi}{N-1}} \times \int_0^{\infty} \int_0^{\infty} \frac{F_0^{(N-1)}(R_\rho^{(N-1)},R_z^{(N-1)}) F_j^{(N)}(R_\rho^{(N)},R_z^{(N)})}{R_\rho^{(N-1)}\sqrt{R_z^{(N-1)}}} \times \left(1 + \frac{1}{N-1}\frac{\rho^2}{R_\rho^{(N-1)2}}\right)^{-(2N-1)/4} \times \left(1 + \frac{1}{N-1}\frac{z^2}{R_z^{(N-1)2}}\right)^{-(N-1)/4} dR_\rho^{(N-1)} dR_z^{(N-1)}, \tag{7}$$

where $r=r^{(N)}$ and

$$\xi = \frac{\Gamma(N)\Gamma\left(\frac{N}{2}\right)}{N^{3/2}\Gamma(N-1)\Gamma\left(\frac{N-1}{2}\right)}.$$

Note Eq. (6) is a generalization of Eq. (3.4) of Ref. [4].

Let us compare in Fig. 4 two sets of "single-particle" functions for $N=100$ and $N=30\,000$, one calculated by the above hyperspherical procedure and the other by the Bogoliubov approximation. Since the Bogoliubov functions come in pairs, corresponding to creation or to destruction of a quasiparticle state, we show what corresponds to the creation on the ρ-z plane with the color coding designed to reflect the relative amplitude inclusive of the sign. The label j is as defined in Fig. 3. We observe an obvious correspondence between χ_j and u_j for $j=1,2$ and for $j=4,5$. The nodal structures indicate that $j=1$ and 3 pertain to the quadrupole and $j=2$ and 5 to the monopole excitations. The clear-cut wedge-like nodal lines for the quadrupole excitation stem from $F_j^{(N)}(R_\rho^{(N)},R_z^{(N)})$ whose characteristic feature is represented for the lowest excitation by the factor of

$$R_\rho^2 - 2R_z^2 = \frac{1}{N}\sum_i (\rho_i^2 - 2z_i^2),$$

which is relevant for the representation of a single-particle excitation function with the quadrupole symmetry. Meanwhile, the topology of χ_3 is markedly distorted from u_3. The Bogoliubov function u_3 shows, by virtue of the number of nodes, that it pertains to the sextupole. In the current setting of calculations, no mechanism is built into the KHA method for representing this type of surface rotation. To remedy this flaw requires us to incorporate additional degrees of freedom into the current representation.

Let us note that the tendency persists at $N=30\,000$, but the hyperspherical χ_j does not contract as dramatically as the Bogoliubov function whose radial extent shows a sharp cutoff of the Thomas-Fermi behavior. Instead, χ behaves as the Gaussian function because of the sharp δ-function-like concentration of F around the equilibrium hyperradius $R=\sqrt{R_\rho^2+R_z^2}=R_0$. Indeed, the ansatz

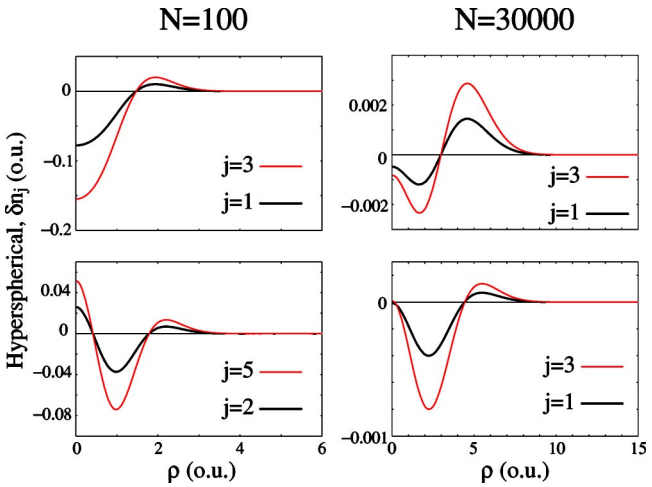

FIG. 5. Slice of the residual density δn at $z=0$ plotted as a function of ρ for $N=100$ and $N=30\,000$. Residual densities δn_1 and δn_4 differ by the factor of 2 and similarly for δn_2 and δn_5. The excitation in the ground state is overwhelmed by the increase in occupancy of the lowest-lying excited state, burying the higher excited states and making their proportion insignificant.

$$|F(R_\rho,R_z)|^2 \propto \delta(R-R_0)$$

substituted into Eq. (6) reduces readily to

$$n_0 \propto \mathrm{e}^{-3r^2/2R_0^2},$$

when $r^2=\rho^2+z^2 \ll NR^2$. Note that since the departure of F from Gaussian behavior can be readily incorporated into the time-dependent Schrödinger equation, the hyperspherical method despite the KHA has flexibility beyond the Gaussian approximation. An example of this flexibility may be found in the treatment of the decay of an attractive BEC to be reported elsewhere.

Let us return to the excitation in the ground-state channel for ^{87}Rb. In addition to u_j and χ_j, Fig. 4 shows $n_j(\rho,z)$, and we observe almost no correspondence between u_j and n_j. Consider the residual single-particle density $\delta n_j(\rho,z)$ which represents the excitation content shorn of the ground-state contribution—namely,

$$\delta n_j(\rho,z) = n_j(\rho,z) - n_0(\rho,z).$$

The dependence of $\delta n_j(\rho,z)$ on j in Fig. 5 suggests that the excitation within the ground-state channel corresponds to an increase in the number of particles in the first excited state. [A more quantitative check based on the integral of $\delta n_j(\rho,z)$ shows that this contention holds to the pursued accuracy.] To make the point clearer, let us presume to represent a state in the number representation such that

$$|N_0,N_1,N_2,\ldots\rangle$$

indicates N_0 (quasi)particles in the ground state, N_1 (quasi)particles in the first excited state of the breathing mode, N_2 (quasi)particles in the second excited state, etc. The hyperradial excitation in a single channel then amounts to generating states $|N-N_1,N_1,0,0,\ldots\rangle$ with increment only in N_1—i.e., with negligible component in higher-excited single-particle states. As seen in Fig. 4, the plots of χ_j indicate the presence of higher-excited single-particle states in the hyperspherical solution. Their magnitudes, though not readily noticeable on the color-coded relative scale, grow smaller as j increase, which fact corroborates the above observation. The higher excited single-particle states are thus buried in the larger background of $|N-N_1,N_1,0,0,\ldots\rangle$.

The current situation may be explained by way of a simple analogy drawn on the role of R^2, the generator of the monopole excitation. Let us liken excitation within the ground-state hyperspherical channel to raising the power of

$$R^2 = (r_1^2 + r_2^2 + \cdots + r_N^2)/N,$$

interpreting R^2 as representing all N particles in the first-excited single-particle state r^2 while $(R^2)^0$ may be considered as the ground state. Now associate the second-excited state to

$$R^4 = \left(\sum_{i=1}^{N} r_i^4 + \sum_{i\neq j}^{N} r_i^2 r_j^2\right) \Big/ N^2,$$

which consists of $N(N-1)/2$ pairs in the first-excited single-particle state and N particles in the second-excited single-particle state. One can proceed to interpret R^{2j} similarly. In this manner, raising the power of R^2 is seen to be dominated by multiples of particles in the first-excited single-particle state, the relative magnitudes of the other components declining by the integer powers of N.

V. CONCLUSION

This paper dealt with the excited states in the ground-state hyperspherical channel using the lowest-order hyperspherical harmonics approximation as in Ref. [4], but with an extension that enabled us to accommodate anisotropy. The dispersion relations of Stringari [19] for the Thomas-Fermi limit followed from the consideration of the Hessian matrix of the hyperspherical effective potential surface. The hyperspherical excitation within the ground-state channel was seen to correspond largely to the increase in occupation number in the lowest single-particle excited state. We also noted that the hyperspherical method based on a single harmonics is a properly quantized version of the Gaussian variational method, however with the added flexibility of representing a wave packet with a single-particle profile noticeably distorted from Gaussian. The projected single-particle wave function χ shows its correspondence with the Bogoliubov function u for monopoles and quadrupoles, but fails for higher multipoles with rotational excitation. A remedy is suggested and is currently pursued.

An immediate extension of the present method is to the study of collapse via two- and three-body recombination processes. Another facet to be readily explored by the present scheme is the normal-mode analysis of a two-component or multicomponent BEC [28].

ACKNOWLEDGMENTS

We thank Dr. T. Kimura of Kanagawa University for useful discussions and encouragement. We also thank H. Ish-

imura for carefully reading the manuscript. We acknowledge that M. Saito's quiet participation brightened the working atmosphere for the present paper. This work was supported in part by a Grant-in-Aid for Scientific Research (C) from the Ministry of Education, Culture, Sports, Science and Technology, Japan, and also in part by the 21st Century COE program on "Coherent Optical Science." T.M. was also supported in part by a Grant-in-Aid for Young Scientist (B) from Japan Society for the Promotion of Science and by a financial aid from the Matsuo Foundation.

APPENDIX: GENERATING FUNCTION METHOD AND MATRIX ELEMENTS

The principal emphasis here is on the method of evaluating integrals on the hypersphere. A demonstrative example evaluates a marginal reduction in the total energy of the BEC. This appendix thus demonstrates inclusion of the interchannel couplings in the hyperspherical method incorporating several lowest totally symmetric hyperspherical harmonics. Various applications are conceivable. The basic idea is to carry out the integrals in two alternative ways, one with respect to the hyperspherical coordinates and the other to the independent particle coordinates, of which the latter gives closed expressions while the former leaves the desired matrix elements undetermined until the term-by-term comparison fixes them.

Basic idea

Consider the matrix element

$$\langle\langle \mathcal{Y}^z_{\{0\}} | \sum_{i>j} \delta(z_i - z_j) | \mathcal{Y}^z_{\{0\}} \rangle\rangle = \frac{|\mathcal{Y}^z_{\{0\}}|^2}{R_z} \int_\Omega \sum_{i>j} \delta\left(\frac{z_i - z_j}{R_z}\right) d\Omega,$$

$\mathcal{Y}^z_{\{0\}}$ being constant. Meanwhile,

$$\langle\langle \mathcal{Y}^z_{\{0\}} | \mathcal{Y}^z_{\{0\}} \rangle\rangle = |\mathcal{Y}^z_{\{0\}}|^2 \int_\Omega d\Omega = 1.$$

In consequence,

$$\langle\langle \mathcal{Y}^z_{\{0\}} | \delta(z_i - z_j) | \mathcal{Y}^z_{\{0\}} \rangle\rangle = \frac{1}{R_z} \frac{\int_\Omega \delta\left(\frac{z_i - z_j}{R_z}\right) d\Omega}{\int_\Omega d\Omega}.$$

To obtain the necessary integrals, consider

$$\begin{aligned}
&\int_V \sum_{i>j} \delta(z_i - z_j) \mathrm{e}^{-R_z^2} dV \\
&= \int_0^\infty N^{N/2} R_z^{N-2} \mathrm{e}^{-R_z^2} dR_z \int_\Omega \sum_{i>j} \delta\left(\frac{z_i - z_j}{R_z}\right) d\Omega \\
&= I_{N-2} \int_\Omega \sum_{i>j} \delta\left(\frac{z_i - z_j}{R_z}\right) d\Omega
\end{aligned}$$

and also

$$\begin{aligned}
\int_V \sum_{i>j} \delta(z_i - z_j) \mathrm{e}^{-R_z^2} dV &= \frac{N(N-1)}{2} \frac{(2I_0)^{N-1}}{\sqrt{2}} \\
&= \frac{N(N-1)}{2} \frac{\pi^{(N-1)/2}}{\sqrt{2}},
\end{aligned}$$

where V stands for the unrestricted N-dimensional space and

$$I_n \equiv \int_0^\infty \xi^n \mathrm{e}^{-\xi^2} d\xi = \frac{1}{2} \Gamma\left(\frac{n+1}{2}\right).$$

Thus,

$$\begin{aligned}
\langle\langle \mathcal{Y}^z_{\{0\}} | \sum_{i>j} \delta(z_i - z_j) | \mathcal{Y}^z_{\{0\}} \rangle\rangle &= \frac{N(N-1)}{2} \frac{2\sqrt{2}}{\pi^{1/2} N^{1/2}} \\
&\times \frac{\Gamma\left(\frac{N}{2}\right)}{\Gamma\left(\frac{N-1}{2}\right)} \frac{1}{R_z}.
\end{aligned}$$

In much the same way, we get

$$\begin{aligned}
&\langle\langle \mathcal{Y}^\rho_{\{0\}} \mathcal{Y}^z_{\{0\}} | \sum_{i>j} \delta(\vec{r}_i - \vec{r}_j) | \mathcal{Y}^\rho_{\{0\}} \mathcal{Y}^z_{\{0\}} \rangle\rangle \\
&= \frac{N(N-1)}{2} \frac{1}{\sqrt{8\pi^3}} \frac{\Gamma(N)\Gamma\left(\frac{N}{2}\right)}{N\Gamma(N-1) N^{1/2} \Gamma\left(\frac{N-1}{2}\right)} \frac{1}{R_\rho^2 R_z}.
\end{aligned}$$

Generating function method

Given this demonstration, it is straightforward to see for the isotropic trap that the following generating functions facilitate to evaluate integrals over the hypersphere involving homogeneous and totally symmetric polynomials of higher degrees, a technique that should be useful in describing low-lying excitations in the hyperspherical approach. We use the following two types of generating function. One is of the Gaussian form and allows for angular correlations (type *A*); the other is designed specifically for the particles in the *s*-state (type *B*).

Type A

Consider the generating function in the form

$$\begin{aligned}
G &\equiv \exp\left\{ -\frac{1}{2} R^2 - s \sum_{i \neq j}^N (\vec{r}_i \cdot \vec{r}_j) \right\} \\
&= \sum_{n=0} R^{2n} \exp\left\{ -\frac{1}{2} R^2 \right\} \phi_n(\Omega) s^n. \qquad \text{(A1)}
\end{aligned}$$

We have

$$\begin{aligned}
\langle G | G \rangle &= \sum_{n,m} I_{2n+2m+3N-1} \mathcal{O}_{nm} s^m t^m = \pi^{3/2} \{1 - (s+t)^{-3(N-1)/2}\} \\
&\times \{(N-1)(s+t) + 1\}^{-3/2},
\end{aligned}$$

where

$$\mathcal{O}_{nm} = \int \phi_n \phi_m d\Omega, \tag{A2}$$

$$\langle G|\sum_{i=1}^{N} \nabla_i^2|G\rangle = \frac{3N}{2}\pi^{3N/2}\{1-(s+t)\}^{-3(N-1)/2}\{(N-1)(s+t) + 1\}^{-3/2}\frac{(N-1)(s^2+t^2)-(N-2)(s+t)-1}{(1-s-t)\{(N-1)(s+t)+1\}}$$
$$= \sum_{n,m}[\{I_{2n+2m+3N+1} - (4m+3N)I_{2n+2m+3N-1} + 2m(2m+3N-2)I_{2n+2m+3N-3}\}\mathcal{O}_{nm} + I_{2n+2m+3N-3}\Lambda_{nm}^2],$$

$$\langle G|\sum_{i>j}\delta(\vec{r}_i-\vec{r}_j)|G\rangle = \frac{N(N-1)}{2}\frac{1}{\sqrt{8}}\pi^{3(N-1)/2}\{1-(s+t)\}^{-3(N-2)/2}\{(N-1)(s+t)+1\}^{-3/2}$$
$$= \sum_{n,m} I_{2n+2m+3N-4}\Delta_{nm}s^n t^m,$$

where Λ_{nm}^2 and Δ_{nm} are the grand angular momentum and interaction matrix elements, respectively:

$$\Lambda_{nm}^2 = \int_{\Omega^{3N-1}} \phi_n(\Omega^{3N-1})\Lambda^2\phi_m(\Omega^{3N-1})d\Omega^{3N-1},$$

$$\Delta_{nm} = \int_{\Omega^{3N-1}} \phi_n(\Omega^{3N-1})\sum_{i>j}\delta(\vec{r}_i-\vec{r}_j)\phi_m(\Omega^{3N-1})d\Omega^{3N-1}.$$

Type B

A particular example here employs a sixth-degree polynomial in the exponent:

$$G \equiv \exp\left\{s\sum_{i=1}^{N} r_i + t\sum_{i=1}^{N} r_i^2 + u\sum_{i=1}^{N} r_i^3 + v\sum_{i=1}^{N} r_i^4 + w\sum_{i=1}^{N} r_i^5 + x\sum_{i=1}^{N} r_i^6 - \frac{1}{2}R^2\right\}$$
$$= \prod_{i=1}^{N}\exp\left\{sr_i + tr_i^2 + ur_i^3 + vr_i^4 + wr_i^5 + xr_i^6 - \frac{1}{2}r_i^2\right\}$$
$$= \sum_{\beta}\frac{R^M}{\prod_{i=1}^{6} n_i!}\phi_\beta(\Omega)\exp\left(-\frac{1}{2}R^2\right)\gamma, \tag{A3}$$

where

$$\gamma = s^{n_1}t^{n_2}u^{n_3}v^{n_4}w^{n_5}x^{n_6},$$

$$M = n_1 + 2n_2 + 3n_3 + 4n_4 + 5n_5 + 6n_6,$$

and β collectively represents $n_1, n_2, n_3, n_4, n_5, n_6$. We have

$$\langle G|G\rangle = \left\{4\pi\sum_{\beta}\sum_{\beta'}\frac{I_{M+M'+2}}{\prod_{i=1}^{6} n_i!\prod_{i=1}^{6} n_i'!}\gamma\gamma'\right\}^N = \sum_{\beta,\beta'} I_{M+M'+3N-1}\mathcal{O}_{\beta,\beta'}\gamma\gamma',$$

$$\langle G|\sum_{i=1}^{N}\nabla_i^2|G\rangle = \sum_{\beta\beta'}\left[\frac{4\pi}{\prod_{i=1}^{6} n_i!\prod_{i=1}^{6} n_i'!}\{M'(M'+1)I_{M+M'} - (2M'+3)I_{M+M'+2} + I_{M+M'+4}\}\right]\gamma\gamma'$$
$$\times\left[4\pi\sum_{\beta,\beta'}\frac{I_{M+M'+2}}{\prod_{i=1}^{6} n_i!\prod_{i=1}^{6} n_i'!}\gamma\gamma'\right]^{N-1}$$
$$= \sum_{\beta,\beta'}[\{M'(M'+3N-2)I_{M+M'+3N-3} - (2M'+3N)I_{M+M'+3N-1} + I_{M+M'+3N+1}\}\mathcal{O}_{\beta,\beta'} - I_{M+M'+3N-3}\Lambda_{\beta,\beta'}]\gamma\gamma',$$

$$\langle G|\sum_{i>j}\delta(\vec{r}_i-\vec{r}_j)|G\rangle = \sum_{\beta}\left[\frac{4\pi 2^{\Sigma_{i=1}^{6}(n_i+n_i')}}{2^{(M+M'+3)/2}\prod_{i=1}^{6} n_i!\prod_{i=1}^{6} n_i'!}I_{M+M'+2}\gamma\gamma'\right]\left[4\pi\sum_{\beta,\beta'}\frac{I_{M+M'+2}}{\prod_{i=1}^{6} n_i!\prod_{i=1}^{6} n_i'!}\gamma\gamma'\right]^{N-2}$$
$$= \sum_{\beta,\beta'}[I_{M+M'+3N-4}\Delta_{\beta,\beta'}\gamma\gamma'].$$

However, no proof or verification is presently given to the plausible completeness of the homogeneous multivariable polynomials produced by this method.

The single-particle integrals in the above expressions can be symbolically expanded on the computer by iteration, and with 8-byte real numbers the matrix elements can be readily extracted for the lowest tens of elements for up to $N=10\,000$ or so.

[1] M. H. Anderson, J. R. Ensher, M. R. Matthews, C. E. Wieman, and E. A. Cornell, Science **269**, 198 (1995); C. C. Bradley, C. A. Sackett, J. J. Tollett, and R. G. Hulet, Phys. Rev. Lett. **75**, 1687 (1995); K. B. Davis, M.-O. Mewes, M. R. Andrews, N. J. van Druten, D. S. Durfee, D. M. Kurn, and W. Ketterle, *ibid.* **75**, 3969 (1995); E. A. Cornell and C. E. Wieman, Rev. Mod. Phys. **74**, 875 (2002).

[2] N. N. Bogoliubov, J. Phys. (Moscow) **11**, 23 (1947).

[3] E. P. Gross, Nuovo Cimento **20**, 454 (1961); J. Math. Phys. **4**, 195 (1963); L. P. Pitaevskii, Pis'ma Zh. Eksp. Teor. Fiz. **40**, 646 (1961) [Sov. Phys. JETP **13**, 451 (1961)].

[4] J. L. Bohn, B. D. Esry, and C. H. Greene, Phys. Rev. A **58**, 584 (1998).

[5] D. Blume and Chris H. Greene, Phys. Rev. A **66**, 013601 (2002).

[6] Professor C. H. Greene kindly brought our attention to the following two articles by Y. E. Kim and A. L. Zubarev: namely, J. Phys. B **33**, 55 (2000) and **33**, 3905 (2000).

[7] J. Macek, J. Phys. B **1**, 831 (1968).

[8] U. Fano, Rep. Prog. Phys. **46**, 97 (1983), and references therein. For an interesting recent application of the hyperspherical method, see V. Kokoouline and C. H. Greene, Phys. Rev. A **69**, 032711 (2004) as well as O. Sørensen, D. V. Fedorov, and A. S. Jensen, *ibid.* **68**, 063618 (2003).

[9] S. Watanabe and C. D. Lin, Phys. Rev. A **36**, 511 (1987); T. Morishita and C. D. Lin, *ibid.* **59**, 1835 (1999); **67**, 022511 (2003).

[10] J. Z. Tang, S. Watanabe, and M. Matsuzawa, Phys. Rev. A **46**, 2437 (1992); C. D. Lin, Phys. Rep. **257**, 1 (1995); S. Watanabe, T. Morishita, D. Kato, O. I. Tolstikhin, K. Hino, and M. Matsuzawa, Nucl. Instrum. Methods Phys. Res. B **124**, 218 (1997); O. I. Tolstikhin, S. Watanabe, and M. Matsuzawa, Phys. Rev. Lett. **74**, 3573 (1995); D. Kato and S. Watanabe, *ibid.* **74**, 2443 (1995); T. Morishita, K. Hino, S. Watanabe, and M. Matsuzawa, Phys. Rev. A **53**, 2345 (1996).

[11] V. M. Pérez-García, H. Michinel, J. I. Cirac, M. Lewenstein, and P. Zoller, Phys. Rev. A **56**, 1424 (1997).

[12] L. Salasnich, A. Parola, and L. Reatto, Phys. Rev. A **69**, 045601 (2004); also S. Stringari, *ibid.* **58**, 2385 (1998).

[13] D. S. Hall, M. R. Matthews, C. E. Wieman, and E. A. Cornell, Phys. Rev. Lett. **81**, 1543 (1998).

[14] H. Saito and M. Ueda, Phys. Rev. Lett. **86**, 1406 (2001); J. Skalski, Phys. Rev. A **65**, 033626 (2002); J. L. Roberts, N. R. Claussen, S. L. Cornish, E. A. Donley, E. A. Cornell, and C. E. Wieman, Phys. Rev. Lett. **86**, 4211 (2001).

[15] D. L. Feder, C. W. Clark, and B. I. Schneider, Phys. Rev. A **61**, 011601 (2000).

[16] Q.-H. Park and J. H. Eberly, Phys. Rev. Lett. **85**, 4195 (2000).

[17] T. Isoshima, M. Nakahara, T. Ohmi, and K. Machida, Phys. Rev. A **61**, 063610 (2000). See also Ref. [28] below.

[18] A. V. Yulin and D. V. Skryabin, Phys. Rev. A **67**, 023611 (2003); A. Trombettoni and A. Smerzi, Phys. Rev. Lett. **86**, 2353 (2001); D. Jaksch, C. Bruder, J. I. Cirac, C. W. Gardiner, and P. Zoller, *ibid.* **81**, 3108 (1998); O. Zobay, S. Pötting, P. Meystre, and E. M. Wright, Phys. Rev. A **59**, 643 (1999).

[19] S. Stringari, Phys. Rev. Lett. **77**, 2360 (1996).

[20] F. Dalfovo, S. Giorgini, M. Guilleumas, L. Pitaevskii, and S. Stringari, Phys. Rev. A **56**, 3840 (1997); B. D. Esry, *ibid.* **55**, 1147 (1997); M. Edwards, P. A. Ruprecht, K. Burnett, R. J. Dodd, and C. W. Clark, Phys. Rev. Lett. **77**, 1671 (1996); P. A. Ruprecht, M. Edwards, K. Burnett, and C. W. Clark, Phys. Rev. A **54**, 4178 (1996).

[21] Here, the unit of length is $\sqrt{\hbar/m\omega}$ and that of energy is $\hbar\omega$.

[22] J. Avery, *Hyperspherical Harmonics: Applications in Quantum Theory* (Kluwer, Dordrecht, 1989) and references therein.

[23] The review article by Fano cited above [8] provides a comprehensive picture of the method up to 1983.

[24] F. Dalfovo, S. Giorgini, L. P. Pitaevskii, and S. Stringari, Rev. Mod. Phys. **71**, 463 (1999); A. J. Leggett, *ibid.* **73**, 307 (2001).

[25] Our numerical method for the GP equation follows the work of B. I. Schneider and D. L. Feder, Phys. Rev. A **59**, 2232 (1999).

[26] D. K. Watson and B. A. McKinney, Phys. Rev. A **59**, 4091 (1999); B. A. McKinney and D. K. Watson, *ibid.* **65**, 033604 (2002).

[27] M. Ueda and A. J. Leggett, Phys. Rev. Lett. **80**, 1576 (1998).

[28] Z.-D. Chen, J.-Q. Liang, S.-Q. Shen, and W.-F. Xie, Phys. Rev. A **69**, 023611 (2004); M. R. Andrews, C. G. Townsend, H.-J. Miesner, D. S. Durfee, D. M. Kurn, and W. Ketterle, Science **275**, 637 (1997).